Interference of photons from independent hot atoms

Jaromír Mika,[1] Stuti Joshi,[1] Lukáš Lachman,[1] Robin Kaiser,[2] and Lukáš Slodička[1,*]
[1]*Department of Optics, Palacký University, 17. listopadu 12, 771 46 Olomouc, Czech Republic*
[2]*Université Côte d'Azur, CNRS, INPHYNI, 17 Rue Julien Lauprête, 06200 Nice, France*

(Received 3 October 2024; accepted 12 December 2025; published 20 January 2026)

The coherence of light from independent ensembles of elementary atomic emitters plays a paramount role in diverse areas of modern optics. We demonstrate the interference of photons scattered from independent ensembles of warm atoms in atomic vapor. It relies on the feasibility of the preservation of coherence of light scattered elastically in the forward and backward directions from Doppler-broadened atomic ensembles, such that photons with chaotic photon statistics from two opposite atomic velocity groups contribute to the same detection mode. While the random phase fluctuations of the scattered light caused by a large thermal motion prevent direct observability of the interference in the detected photon rate, the stable frequency difference between photons collected from scattering off counterpropagating laser beams provides strong periodic modulation of the photon coincidence rate with the period given by the detuning of the excitation laser from the atomic resonance. The presented interferometry represents a sensitive and robust methodology for Doppler-free optical atomic and molecular spectroscopy based on photon correlation measurements on scattered light.

DOI: 10.1103/r5n8-pt1g

I. INTRODUCTION

Optical coherence is paramount to all areas of modern optics. The feasibility of the coherence of light scattered from atoms enabled a broad range of essential applications ranging from optical atomic and molecular spectroscopy to diverse atomic sensors, efficient light-matter interfaces, and long-distance quantum communication [1–6]. The corresponding experimental approaches and their theoretical analysis consistently acknowledge severely detrimental impact of thermal atomic motion as a predominant source of decoherence [7–14]. The usual approaches toward mitigation of its impact correspond to suppression of thermal kinetic energy by means of laser cooling, the employment of tight atomic trapping potentials, optimized excitation geometries, or diverse spatial and spectral filtering schemes for minimization of the which-way information due to atomic recoils.

We propose and demonstrate the availability of preservation of optical coherence in the high-temperature limit of atomic scatterers by developing a scheme for generation and observation of the interference of light scattered from independent ensembles of atoms at room temperature. The observability of interference fringes is enabled by a broad spectral distribution of thermal atoms at high temperatures and employs a natural atomic velocity selectivity of photon scattering in a weak excitation regime [15]. Excitation using a single laser beam in the retroreflected spatial configuration allows for indistinguishable generation and observation of photons at two well-defined frequencies separated by the stable relative difference determined by the excitation laser detuning Δ_L from the atomic resonance. Due to the low phase-space density of the generated single-photon level light emerging from fast and inherently random processes related to the thermal atomic motion, the direct observation of the corresponding first-order interference is not feasible [16–18]. However, photons produced from such intrinsically independent sources can manifest the presence of transient interference visible in the second-order correlation function [19–30].

We demonstrate the coherence of light scattering in hot atomic vapors within a broad range of detunings from atomic resonance with a positive contribution of different atomic velocity classes. The coherence can be maintained both in the forward and in the backward scattering, where the latter provides a stable frequency difference between the scattered fields and the employed atomic transition. The verification of coherence using the interferometric scheme, including light fields scattered from counterpropagating excitation laser beams, reveals intrinsic application in atomic spectroscopy. The methodology is based on the measurement of atomic fluorescence in photon correlation signal and allows for a sub-Doppler spectroscopy in low optical depth regime applicable to dilute ensembles of hot atoms. It allows for a direct estimation of the absolute value of the laser detuning from atomic resonance without any need for the modulation of the laser probe frequency or atomic transition parameters, and neither requires calibration of any interaction parameters or thermal atomic motion.

II. INTERFEROMETRY WITH HOT ATOMIC SCATTERERS

The principle of the interferometric scheme is depicted in Fig. 1. The excitation laser beam with a wave vector $\mathbf{k}_{L_1}$ and

*Contact author: slodicka@optics.upol.cz

Published by the American Physical Society under the terms of the Creative Commons Attribution 4.0 International license. Further distribution of this work must maintain attribution to the author(s) and the published article's title, journal citation, and DOI.

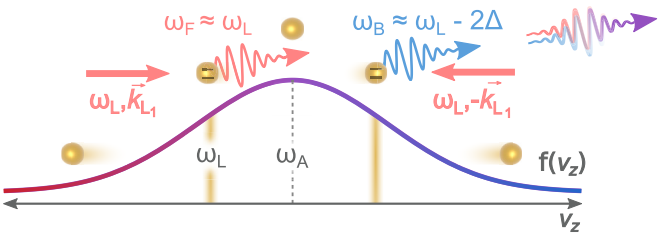


FIG. 1. The principle of interference of light from independent warm atomic ensembles. The laser at the frequency ω_L is detuned by Δ from the atomic transition ω_A and scatters off the particular velocity class of atoms that follow the thermal velocity distribution $f(v)$ along the laser propagation axis. In the forward scattering (F), the corresponding Doppler shift effectively compensates. The retroreflected laser scatters off atoms possessing the opposite direction of motion but with the same velocity magnitude. The corresponding backward-scattered photons (B) are frequency shifted by $\approx \Delta$ concerning an observer in the frame moving with the atomic scatterer and by approximately 2Δ to the forward-scattered photons.

frequency ω_L is detuned from the atomic transition ω_A by Δ and elastically scatters from hot thermal atoms with the particular projection of atomic velocity to the direction of the excitation laser $\mathbf{v}_z$, which fulfills $\mathbf{k}_{L_1} \cdot \mathbf{v} \approx \Delta$.

The photons with a wave vector $\mathbf{k}_F$ scattered in close to a forward (F) direction at an angle $\theta \to 0$ retain the central frequency of the laser $\omega_F = \omega_L + (\mathbf{k}_{L_1} - \mathbf{k}_F) \cdot \mathbf{v} \approx \omega_L$. The standard deviation of their Gaussian spectral distribution corresponds to $\sigma_F = \sigma_{\omega,D} \sin\theta$, where $\sigma_{\omega,D}$ is the width of the complete frequency redistributed spectrum for photon scattered in warm atomic vapor [15,31,32]. The scattered light is expected to present chaotic statistics with nearly ideal photon bunching $g^{(2)}(0) \approx 2$ in the single-mode detection regime [33]. The second interferometer path is implemented by scattering the retroreflected excitation laser with $\mathbf{k}_{L_2} = -\mathbf{k}_{L_1}$, which interacts with atoms with exactly opposite velocity direction $-\mathbf{v}_z$. Photons scattered backward (B) with a wave vector $\mathbf{k}_B$ at an angle $\theta \to \pi$ toward the same detector will acquire the frequency $\omega_B = \omega_L + (\mathbf{k}_{L_2} - \mathbf{k}_B) \cdot \mathbf{v}$, which means a frequency difference of $(\mathbf{k}_{L_2} - \mathbf{k}_B) \cdot \mathbf{v} \approx 2\Delta$ to the forward scattered part. Their spectral width results from the residual Doppler broadening for scattering at the angle $\theta + \pi$ and an additional term stemming from the longitudinal part of the velocity distribution $f(v_z)$ of contributing atoms. In a low saturation limit, it corresponds to the natural linewidth Γ of the atomic transition. The total spectral width of backscattered light then approximately results in $\sigma_B \approx \sqrt{(\sigma_{\omega,D} \sin\theta)^2 + (2\Gamma)^2}$, where the factor of 2 comes from the sum of the two equal Doppler shifts in the excitation and emission processes [15]. The fluctuating positions of atomic scatterers with Brownian motion prevent direct observability of interference of weak photon signals scattered from independent atoms in the detected photon rate. However, the stable frequency difference between forward- and backward-scattered fields can provide visible interference in the second-order correlations $g^{(2)}(\tau)$ with the characteristic beating with a period of $1/(2\Delta)$ [19]. The oscillations of photon correlations become observable for any detunings Δ in the range $\sigma_{\omega,D} > \Delta > \sigma_F, \sigma_B$. The upper limit is set by the width of the Doppler-broadened atomic spectra $\sigma_{\omega,D}$. The lower is given by the requirement on observation of modulation within the coherence time given by the residual Doppler broadening corresponding to σ_F and σ_B or frequency difference to other electronic levels in hyperfine manifolds. Note that in addition to these fundamental limitations, particular technological constraints, including especially the temporal resolution of the employed photon detectors, or the overall detection efficiency, will set the upper limit on observable beating frequency 2Δ.

The single-mode optical field resulting from scattering on the two atomic velocity classes corresponding to the forward- and backward-scattered light can be expressed as

$$E(t) \propto \sum_{i=1}^{N} E_{F,i} e^{-i(\omega_{F,i} t - \mathbf{k}_F \cdot \mathbf{r}_i)} + \sum_{j=1}^{N} E_{B,j} e^{-i(\omega_{B,j} t - \mathbf{k}_B \cdot \mathbf{r}_j)}, \quad (1)$$

where $E_{F,i(B,j)}$ are the amplitudes of the fields from $i(j)$th atom and $\mathbf{r}$ are the position vectors of atoms. The summation includes contributions from a large number of $N \gg 1$ atoms in each of the two opposite atomic velocity classes. Here, we assume that the numbers of contributing atoms to the forward- and backward-scattered fields are approximately the same with relevance to the presented experimental configuration, where the numbers of contributing atoms are given by the observation volume of the two atomic ensembles with the same atomic density. The Doppler distribution of atomic velocity classes of thermal vapor affects the number of contributing atoms in both ensembles equally, as the effective laser detuning from atomic resonance is the same for both scattering contributions. The evaluation of the normalized second-order correlation function in the limit of thermally fluctuating atomic positions gives

$$g^{(2)}(\tau) = 1 + \frac{1}{(\bar{n}_F + \bar{n}_B)^2} \left| \bar{n}_F g_F^{(1)}(\tau) + \bar{n}_B g_B^{(1)}(\tau) e^{i(\omega_F - \omega_B)\tau} \right|^2. \quad (2)$$

Here, the first-order temporal correlation functions $g^{(1)}_{F,B}(\tau)$ reflect the coherence of light scattered on the individual atomic ensembles. The term $\bar{n}_{F(B)}$ corresponds to mean photon number from a particular atomic ensemble, which can be affected by different atomic level populations and losses experienced by the two fields. The complete derivation can be found in the Supplemental Material [34], which includes Refs. [31,35]. The equation reveals the crucial contribution of beating of the first-order correlation functions $g^{(1)}(\tau)$, which modulates the second-order photon correlations at their mean frequency difference $\omega_F - \omega_B$. It represents an extended version of the Siegert relation for chaotic light with two contributing atomic thermal light sources at different frequencies [35]. The visibility of the beating of first-order coherences can be controlled by the relative contributions of two atomic velocity classes, which depend on the amount of detected forward- and backward-scattered light. For equal number of photons from the two atomic velocity classes contributing to the signal, the contrast is maximal. We emphasize that the resonant nature of the interaction is essential for the velocity selectivity of scatterers, as assumed in Eq. (1). Consequently, high visibility of interference requires $(\omega_F - \omega_B) \approx 2\Delta > \sigma_F, \sigma_B$, such that the emitted photons correspond to different

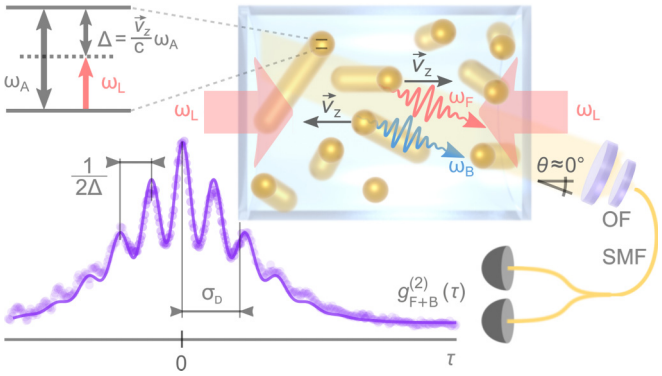


FIG. 2. Experimental scheme and example measurement of interference of light from warm atomic vapors. The scattering of two counterpropagating laser beams off the particular velocity classes of atoms results in forward (F)- and backward (B)-scattered photons with a frequency difference of $\approx 2\Delta$ collected in the same optical mode defined by the single-mode optical fiber (SMF). The measurement of the second-order correlations $g^{(2)}(\tau)$ provides coherent frequency beating with a period of $1/(2\Delta)$. The additional optical filtering (OF) in the detection path suppresses various noise contributions. Its detailed specification can be found in Supplemental Material [34].

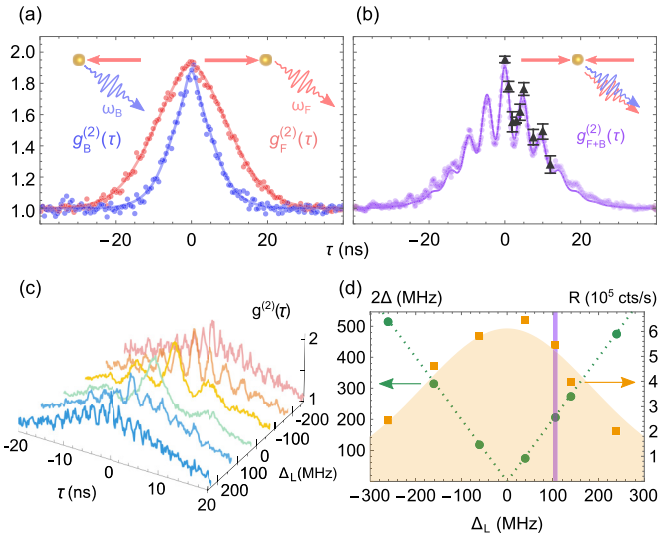


FIG. 3. Panel (a) shows the measurements of the individual $g^{(2)}_{\mathrm{F(B)}}(\tau)$ for photons emitted from two different velocity classes of ensembles of warm atoms. The corresponding $g^{(2)}_{\mathrm{F+B}}(\tau)$ emerging from their interference is shown in panel (b). The fit of the interference pattern uses Eq. (2), where $\bar{g}^{(1)}(\tau)$ of atoms from the two atomic ensembles are taken from their independent measurements. The evaluation of particular $g^{(2)}(\tau)$ data points using the Siegert relation from the independently measured $|g^{(1)}(\tau)|^2 + 1$ is shown with black triangles. The error bars depict a single standard deviation. Graph in panel (c) summarizes measurements of $g^{(2)}(\tau)$ for different laser detunings Δ_{L}. The evaluated mean modulation frequencies f_{mod} from a direct Fourier analysis are shown in panel (d). Here, green dotted lines illustrate its linear dependence on independently measured detuning Δ_{L}. The stability of such frequency estimation is practically limited by detected photon rates shown as orange data points. The filled area depicts the corresponding simulation considering the atomic populations at different velocity classes with a Gaussian uncertainty of the Doppler broadened spectra σ_{DB}, including also the residual modification due to the Fabry-Pérot spectral filter. The marked data point corresponds to the measurement presented in panel (b).

nonoverlapping spectral components with width given by the residual Doppler broadening.

III. EXPERIMENTAL DEMONSTRATION

The experimental demonstration of the scheme for observation of interference from independent warm atoms employs the excitation of warm ^{87}Rb vapor using a single laser beam in a retroreflected standing-wave configuration, as displayed in Fig. 2. A collimated Gaussian laser beam has a radius of $w_{\mathrm{E}} = 1.1 \pm 0.1$ mm and frequency detuning Δ_{L} from the $5\mathrm{S}_{1/2}(F = 2) \leftrightarrow 5\mathrm{P}_{3/2}(F' = 3)$ transition. The optical power of the transmitted laser of 50 μW measured at the output of the cell along the forward-scattering direction corresponds to the excitation in a regime far from saturation. The standing-wave configuration is achieved by the reflection from the planar mirror behind the cell. The excitation and observation optical modes overlap in the proximity of the cell output viewport, which reduces photon losses for both interfering channels. The forward-scattered photons are observed under the small angle $\theta = 2^\circ \pm 0.5^\circ$. The backward-scattered photons are collected into the same spatial mode secured by coupling to a single-mode optical fiber. The observation spatial Gaussian mode waist of $w_0 = 95 \pm 5$ μm is positioned at the intersection with the excitation beam. The collected photons pass the polarization filter optimized for maximal transmission of the same circular polarization as the forward-propagating excitation laser beam. We note that the selection of this particular polarization mode is not unique to the functioning of the scheme and it has been successfully tested also for linear polarization mode with similar results. Fabry-Pérot frequency filter is set up to suppress any residual light originating from Raman scatterings to the $F = 1$ state manifold. A balanced set of two single-photon counting modules (SPCMs) in a Hanbury-Brown-Twiss arrangement is employed for the analysis of the second-order photon correlations. The detection setup is assembled such that it provides the feasibility of simultaneous measurement of the modulus of the first-order coherence $|g^{(1)}(\tau)|$ in a Michelson interferometer (see the Supplemental Material [34]).

Examples of the measured interference of light from independent warm atomic ensembles are shown in Fig. 3. The independent photon correlation measurements of forward- and backward-scattered fields for laser detuning $\Delta_{\mathrm{L}} \approx 100$ MHz in panel (a) demonstrate close-to-ideal bunching values $g^{(2)}_{\mathrm{F}}(0) = 1.94 \pm 0.02$ and $g^{(2)}_{\mathrm{B}}(0) = 1.92 \pm 0.03$, emerging from the random phase shifts of scattered photons caused by the large thermal motion of atoms [33,35,36]. Importantly, these individual correlation functions demonstrate large temporal coherences corresponding to spectral bandwidths $\sigma_{\mathrm{F}} \approx 9.6$ MHz and $\sigma_{\mathrm{B}} \approx 15.8$ MHz, respectively. They effectively correspond to average rates of random phase changes in each of the atomic ensembles and set an upper limit on the observable period of interference modulation in the corresponding $g^{(2)}_{\mathrm{F+B}}(\tau)$. The spectral widths agree with their independent evaluations within the uncertainty of

measurement of the scattering angle θ and confirm the predicted scaling of temporal coherence for the backward-scattered signal. We note that the presented backscattering measurements correspond to a first experimental study of $g^{(2)}_{\mathrm{B}}(\tau)$ from warm atoms in such configuration and provide an important confirmation of the feasibility of coherence of light in this direction. The plot in panel (b) depicts the corresponding $g^{(2)}_{\mathrm{F+B}}(\tau)$, where both forward- and backward-scattered fields contribute simultaneously. The interference results in clear modulation of photon coincidence detection probabilities for $|\tau| > 0$ with the period of $f_{\mathrm{mod}} = 210.8 \pm 1.2$ MHz, in agreement with the independently set laser detuning from the $F = 2 \leftrightarrow F' = 3$. The periodic modulation between constructive and destructive interference at the frequency difference of interfering photons signifies the fulfillment of the critical conditions for the presented scheme. It confirms the sufficiency of the velocity selectivity in the given excitation regime and, at the same time, the mutually coherent contribution with sufficient coherence time from atoms at different velocity classes in a strongly Doppler-broadened thermal atomic ensemble. The detected mean photon rate for presented excitation conditions was $R_{(\mathrm{F+B})} = (64 \pm 2) \times 10^4$ counts/s. The measured photon bunching at zero time delay $g^{(2)}_{\mathrm{F+B}}(0) = 1.96 \pm 0.01$. It allows for evaluating an upper limit on the ratio $r = 0.02 \pm 0.005$ between the mean photon number of the residual phase-correlated light and the light from the two independent chaotic light sources with mutually randomized phases. The derivation of the simple model for quantifying residual phase correlations can be found in the Supplemental Material [34]. The rate of simultaneous detection of two photons $R_{\mathrm{C}} = (4.9 \pm 0.3) \times 10^3$ coincidences/s for the time bin of 14.3 ns.

A complementary perspective on the emergence of the modulation of photon bunching can be obtained from the measurement of a first-order correlation function. The corresponding beating can still be observed in the $|g^{(1)}(\tau)|$ evaluated from the measured visibilities of the field autocorrelation measurement. However, rather than emerging from a direct phase interference between the photons emitted from the two disparate atomic velocity classes, the oscillations in $|g^{(1)}(\tau)|$ result from a periodic rephasing of the self-interference of these two independent narrow-band fields for different relative time delays in the interferometer. The $g^{(2)}(\tau)$ evaluated from the measured $|g^{(1)}(\tau)|$ using a Siegert relation [35,37] shown as black triangle data points in Fig. 3 is in agreement with the independently measured second-order correlations within statistically estimated measurement uncertainties.

The fit of the data in Fig. 3(b) using the model based on Eq. (2) confirms that the interference visibility of 32% ± 1% is indeed determined by the relative difference in probabilities of detection of the forward- to backward-scattered photons. The corresponding photon rates were estimated from fit to $R_{\mathrm{F}} = (54 \pm 2) \times 10^4$ counts/s and $R_{\mathrm{B}} = (10 \pm 0.8) \times 10^4$ counts/s. When comparing to more than 2 orders of magnitude faster random phase changes in both modes $\sigma_{\mathrm{F}}, \sigma_{\mathrm{B}}$, this further validates the regime of interference between phase randomized photons. The large difference in the photon rates corresponds to the smaller intensity of the backscattering laser beam, which experiences additional attenuation in the optically dense atomic sample before reaching the observed interaction volume in the cell. We note that the feasibility of the modification of contributing photon rates by changing the polarization settings of the excitation beams and observation mode was tested, which allowed for observation of a high-visibility interference. We also tested the experimental geometry, where the transversal position shift of the excitation beam on the scale much beyond the beam diameter preserves the observability of the interference, which provides complementary proof of the independence of the two contributing atomic ensembles.

The presented interferometry has intrinsic potential for diverse applications in spectroscopy. It can be readily applied for a direct precise estimation of an absolute value of the relative frequency detuning between the excitation laser and internal atomic transition. The photon-correlation detection allows for direct measurement of the absolute value of laser detuning Δ from the Fourier analysis of $g^{(2)}(\tau)$ with a subnatural linewidth precision. The estimation should also include the corresponding residual systematic shift of the beating frequency $f_{\mathrm{mod}} = |\omega_{\mathrm{F}} - \omega_{\mathrm{B}}| = |\omega_L + \Delta(1 - \cos\theta)) - (\omega_L + \Delta(1 + \cos(\theta + \pi))| = 2\Delta\cos\theta$. The experimental geometry presented here with $\theta = 2^\circ \pm 0.5^\circ$ implies a relative shift in the estimated frequency difference on the order of 10^{-4}. Figure 3(c) presents the series of measured $g^{(2)}(\tau)$ with emergent linear dependence of the modulation frequency f_{mod} on the independently estimated laser detuning Δ_{L}. Here, Δ_L was measured on the optical wave meter, with measured short-term instability below $\sigma \approx 1$ MHz. The linear fit using $f_{\mathrm{mod}} = |\alpha\Delta_{\mathrm{L}}|$ provides $\alpha = 1.995 \pm 0.003$, with no apparent deviation from linearity in the measured range within experimental error bars. The evaluations of larger statistical sets at this particular setting corresponding to an average count rate of $(640 \pm 30) \times 10^3$ counts/s provide rapid enhancement of stability for short measurement timescales, in close agreement with the $1/\sqrt{T}$ scaling, where T is the averaging period. The stability of 0.3 ± 0.1 MHz has been reached for $T = 45$ s. The sampling resolution of the Fourier spectra is given by the maximal evaluated $\tau_{\mathrm{max}} = 3.2\,\mu$s and corresponds to 0.154 MHz. The actual feasible frequency resolution is determined by the inverse of the coherence time of contributing photons. In the time domain, the temporal resolution of frequency estimation is set by the acquisition time necessary for achieving desired measurement stability, which is practically limited by the detectable photon rates. It severely decreases for large Δ, which relies on the scattering of atoms from marginal velocity classes. The technical upper limit on the measurement bandwidth is set by the temporal jitter of the employed SPCMs with the average of 500 ± 100 ps.

IV. CONCLUSIONS

The presented experimental methodology provides an exclusive tool for observation of the emergence of coherence of light from independent ensembles of elementary atomic scatterers. It is directly applicable in a broad range of fundamental interferometric tests and in applications in optical atomic and molecular spectroscopy [1,38–41]. It can be implemented to different classical or quantum scatterers with feasible

resonant interaction, independently of the availability of their motional cooling. Importantly, contrary to the broad range of spectroscopy methods based on a free-space laser absorption with sub-Doppler resolution applicable to warm atoms, the presented interference scheme allows for implementation with small samples of atomic or molecular vapors and with electronic transitions providing only very low resonant optical depth. Despite operating in a small saturation parameter limit, the resonant character of interaction is indispensable for its functioning, as it provides the necessary selectivity of velocity classes of contributing scatterers. For atoms, the observation of interference can thus be considered as a unique signature of the quantized internal structure in the elastic scattering limit. Importantly, the interference is not compromised by the large thermal motion. On the contrary, it enables a large measurement bandwidth of atomic spectroscopy. The combination of a high atomic velocity selectivity and photon correlation detection provides sub-Doppler and subnatural linewidth precision in the regime of large thermal motion with demonstrated feasibility of implementation at the single-photon level. The high atomic temperature enhances the spectral bandwidth of the spectroscopy, which differentiates from other laser spectroscopy methods applicable to hot atoms [1]. While the temporal resolution and stability of frequency estimation could in the presented example benefit from the large number of Rb atoms in a vapor cell, the scheme can be particularly useful for analysis of extremely small and dilute atomic or molecular samples due to its intrinsic stability stemming from the observation of the interference signal in second-order correlations. In contrast to the schemes employing direct observation of the first-order interference, the presented methodology is not affected by slow phase drifts of the excitation laser and of interfering signals. These features promise direct applicability for precision optical spectroscopy of dipole transitions of atomic vapors including only about 10^5 atoms in the observation mode, which has the potential to enhance laser spectroscopy of diverse rare atomic isotopes with applicable energy level structure, for example, ^{46}Ca, with relevance to applications [42,43]. Extensions of presented elementary examples to atoms or molecules with closely spaced electronic level manifolds can result in complex beating structures providing information about the contributing energy level structure.

ACKNOWLEDGMENTS

S.J. and J.M. acknowledge the support of the Czech Science Foundation under Project No. GA21-13265X. L.L. acknowledges the support from the Czech Science Foundation (Grant No. 23-06015O). L.S. is grateful for the national funding from the MEYS under Project No. CZ.02.01.01/00/22_008/0004649 (QUEENTEC). L.S. and R.K. acknowledge funding from the QUANTERA ERA-NET cofund in quantum technologies implemented within the European Union's Horizon 2020 Programme (PACE-IN, 8C20004, ANR19-QUAN-003-01). L.S. is grateful to Romain Bachelard for stimulating discussions.

DATA AVAILABILITY

Original experimental data that support the findings of this article can be found in Ref. [44].

[1] S. Svanberg, *Atomic and Molecular Spectroscopy* (Springer, Berlin, Heidelberg, 2001).

[2] L.-M. Duan, M. D. Lukin, J. I. Cirac, and P. Zoller, Long-distance quantum communication with atomic ensembles and linear optics, Nature (London) **414**, 413 (2001).

[3] M. Lukin, *Colloquium:* Trapping and manipulating photon states in atomic ensembles, Rev. Mod. Phys. **75**, 457 (2003).

[4] N. Sangouard, C. Simon, H. De Riedmatten, and N. Gisin, Quantum repeaters based on atomic ensembles and linear optics, Rev. Mod. Phys. **83**, 33 (2011).

[5] C. L. Degen, F. Reinhard, and P. Cappellaro, Quantum sensing, Rev. Mod. Phys. **89**, 035002 (2017).

[6] T. Chanelière, G. Hétet, and N. Sangouard, Quantum optical memory protocols in atomic ensembles, in *Advances in Atomic, Molecular, and Optical Physics*, edited by E. Arimondo, L. F. DiMauro, and S. F. Yelin (Academic Press, New York, 2018), Vol. 67, pp. 77–150.

[7] H. Carmichael, Coherence and decoherence in the interaction of light with atoms, Phys. Rev. A **56**, 5065 (1997).

[8] Z. Ficek and S. Swain, *Quantum Interference and Coherence: Theory and Experiments* (Springer, New York, 2005).

[9] C.-W. Chou, H. De Riedmatten, D. Felinto, S. V. Polyakov, S. J. Van Enk, and H. J. Kimble, Measurement-induced entanglement for excitation stored in remote atomic ensembles, Nature (London) **438**, 828 (2005).

[10] P. Maunz, D. Moehring, S. Olmschenk, K. C. Younge, D. Matsukevich, and C. Monroe, Quantum interference of photon pairs from two remote trapped atomic ions, Nat. Phys. **3**, 538 (2007).

[11] J. Eschner, C. Raab, F. Schmidt-Kaler, and R. Blatt, Light interference from single atoms and their mirror images, Nature (London) **413**, 495 (2001).

[12] T. Legero, T. Wilk, M. Hennrich, G. Rempe, and A. Kuhn, Quantum beat of two single photons, Phys. Rev. Lett. **93**, 070503 (2004).

[13] P. Qian, Z. Gu, R. Cao, R. Wen, Z. Ou, J. Chen, and W. Zhang, Temporal purity and quantum interference of single photons from two independent cold atomic ensembles, Phys. Rev. Lett. **117**, 013602 (2016).

[14] V. Fedoseev, H. Lin, Y.-K. Lu, Y. K. Lee, J. Lyu, and W. Ketterle, Coherent and incoherent light scattering by single-atom wavepackets, Phys. Rev. Lett. **135**, 043601 (2025).

[15] I. G. Hughes, Velocity selection in a Doppler-broadened ensemble of atoms interacting with a monochromatic laser beam, J. Mod. Opt. **65**, 640 (2018).

[16] L. Mandel and E. Wolf, Coherence properties of optical fields, Rev. Mod. Phys. **37**, 231 (1965).

[17] U. Fano, Quantum theory of interference effects in the mixing of light from phase-independent sources, Am. J. Phys. **29**, 539 (1961).

[18] T. Jordan and F. Ghielmetti, Quantum theory of interference of light from two lasers, Phys. Rev. Lett. **12**, 607 (1964).
[19] L. Mandel, Quantum theory of interference effects produced by independent light beams, Phys. Rev. **134**, A10 (1964).
[20] A. T. Forrester, R. A. Gudmundsen, and P. O. Johnson, Photoelectric mixing of incoherent light, Phys. Rev. **99**, 1691 (1955).
[21] G. Magyar and L. Mandel, Interference fringes produced by superposition of two independent maser light beams, Nature (London) **198**, 255 (1963).
[22] M. S. Lipsett and L. Mandel, Coherence time measurements of light from Ruby optical masers, Nature (London) **199**, 553 (1963).
[23] R. L. Pfleegor and L. Mandel, Interference of independent photon beams, Phys. Rev. **159**, 1084 (1967).
[24] Y.-H. Zhai, X.-H. Chen, and L.-A. Wu, Two-photon interference with two independent pseudothermal sources, Phys. Rev. A **74**, 053807 (2006).
[25] J. Liu, Y. Zhou, F.-l. Li, and Z. Xu, The second-order interference between laser and thermal light, Europhys. Lett. **105**, 64007 (2014).
[26] J. Liu, D. Wei, H. Chen, Y. Zhou, H. Zheng, H. Gao, F.-L. Li, and Z. Xu, Second-order interference of two independent and tunable single-mode continuous-wave lasers, Chin. Phys. B **25**, 034203 (2016).
[27] S. Zhang, F. Raza, I. Ahmed, W. Li, K. Jin, and Y. Zhang, Photon interference of second- and third-order correlation generated by two fluorescence sources, J. Phys. Commun. **3**, 095003 (2019).
[28] H. Kim, D. Kim, J. Park, and H. S. Moon, Hong–Ou–Mandel interference of two independent continuous-wave coherent photons, Photonics Res. **8**, 1491 (2020).
[29] A. Romanova, K. Katamadze, G. Avosopiants, L. Biguaa, N. Skryabin, A. Kalinkin, I. Dyakonov, Y. Bogdanov, and S. Kulik, Time-domain Hong–Ou–Mandel interference of quasi-thermal fields and its application in linear optical circuit characterization, Opt. Lett. **47**, 4708 (2022).
[30] L.-Q. Chen, C.-l. Bian, G.-W. Zhang, Z. Ou, and W. Zhang, Observation of temporal beating in first- and second-order intensity measurement between independent Raman Stokes fields in atomic vapor, Phys. Rev. A **82**, 033832 (2010).
[31] A. Dussaux, T. Passerat de Silans, W. Guerin, O. Alibart, S. Tanzilli, F. Vakili, and R. Kaiser, Temporal intensity correlation of light scattered by a hot atomic vapor, Phys. Rev. A **93**, 043826 (2016).
[32] Y. Zhan, J. Zhang, S. Zhang, S. Gong, and Y. Niu, Room-temperature optical non-reciprocity in a Doppler-broadened medium, Opt. Express **33**, 4491 (2025).
[33] M. Morisse, S. Joshi, J. Mika, J. Capella, R. Kaiser, R. Bachelard, L. Slodička, and M. Hugbart, Temporal coherences of atomic chaotic light sources: The Siegert relation and its generalisation to higher-order correlation functions, Europhys. Lett. **147**, 15001 (2024).
[34] See Supplemental Material at http://link.aps.org/supplemental/10.1103/r5n8-pt1g for detailed experimental setup description, full derivation of second-order coherence from warm atoms, description of the model of radiation with partial phase correlations, and detailed second-order correlation functions for various detunings.
[35] R. Loudon, *The Quantum Theory of Light* (Oxford University Press, Oxford, 2000).
[36] J. Mika, L. Podhora, L. Lachman, P. Obšil, J. Hloušek, M. Ježek, R. Filip, and L. Slodička, Generation of ideal thermal light in warm atomic vapor, New J. Phys. **20**, 093002 (2018).
[37] A. Eloy, Z. Yao, R. Bachelard, W. Guerin, M. Fouché, and R. Kaiser, Diffusing-wave spectroscopy of cold atoms in ballistic motion, Phys. Rev. A **97**, 013810 (2018).
[38] W. Demtröder, *Laser Spectroscopy 2: Experimental Techniques* (Springer, Berlin, Heidelberg, 2015).
[39] A. D. Ludlow, M. M. Boyd, J. Ye, E. Peik, and P. O. Schmidt, Optical atomic clocks, Rev. Mod. Phys. **87**, 637 (2015).
[40] D. Pizzey, J. Briscoe, F. Logue, F. Ponciano-Ojeda, S. Wrathmall, and I. Hughes, Laser spectroscopy of hot atomic vapours: from 'scope to theoretical fit', New J. Phys. **24**, 125001 (2022).
[41] K. Jensen, M. Zugenmaier, J. Arnbak, H. Stærkind, M. V. Balabas, and E. S. Polzik, Detection of low-conductivity objects using eddy current measurements with an optical magnetometer, Phys. Rev. Res. **1**, 033087 (2019).
[42] R. F. Garcia Ruiz, M. Bissell, K. Blaum, A. Ekström, N. Frömmgen, G. Hagen, M. Hammen, K. Hebeler, J. Holt, G. Jansen, *et al.*, Unexpectedly large charge radii of neutron-rich calcium isotopes, Nat. Phys. **12**, 594 (2016).
[43] C. Solaro, S. Meyer, K. Fisher, J. C. Berengut, E. Fuchs, and M. Drewsen, Improved isotope-shift-based bounds on bosons beyond the standard model through measurements of the $^2D_{3/2}$-$^2D_{5/2}$ interval in Ca^+, Phys. Rev. Lett. **125**, 123003 (2020).
[44] J. Mika, S. Joshi, L. Lachman, R. Kaiser, and L. Slodička, Experimental data for "Interference of photons from independent hot atoms", Zenodo (2025), https://zenodo.org/records/18004363.